Geobios 81 (2023) 167–177

Contents lists available at ScienceDirect

Geobios

journal homepage: www.elsevier.com/locate/geobio

Ferruginous biolaminations within the pre-Hirnantian (Late Ordovician) of the Carnic Alps, Austria ☆

Annalisa Ferretti [a,*], Frédéric Foucher [b], Frances Westall [b], Luca Medici [c], Barbara Cavalazzi [b,d,e,*]

[a] Department of Chemical and Geological Sciences (DSCG), University of Modena and Reggio Emilia, 41125 Modena, Italy
[b] Centre de Biophysique Moléculaire-CNRS, 45071 Orléans cedex 2, France
[c] National Research Council of Italy, Institute of Methodologies for Environmental Analysis, 85050 Tito Scalo (Potenza), Italy
[d] Department of Biological, Geological, and Environmental Sciences (BiGeA), University of Bologna, 40126 Bologna, Italy
[e] Department of Geology, University of Johannesburg, Johannesburg, South Africa

ARTICLE INFO

Article history:
Received 29 July 2022
Revised 2 November 2022
Accepted 28 January 2023
Available online 29 April 2023

Keywords:
Microstromatolites
Chamosite
Goethite
Uqua Formation
Cellon section

ABSTRACT

Well preserved laminated structures occur within the Upper Ordovician of the Cellon section in the Carnic Alps (Austria), a world-famous reference section for Silurian conodont biostratigraphy. Microfacies from the Upper Ordovician Uqua Formation were characterised by using optical and scanning electron microscopy (SEM), an environmental scanning electron microscopy coupled with microanalyses (SEM/ESEM-EDX) and a confocal laser Raman microscopy. Ferruginous laminated structures overgrowing specific skeletal fragments occur in the lower part of the studied unit in the form of finely red-to greenish coatings composed of chamosite and goethite alternating with calcite bands. Laminae have arborescent to dendrolitic morphologies. Such morphologies suggest a biomediated genesis and the existence of a potential microbial factory acting in a nearby location from which coated material was later redeposited. These ferruginous coatings around organisms are not documented within the latest Ordovician Plöcken Formation at Cellon or in the coeval Wolayer Formation elsewhere.

1. Introduction

The Carnic Alps have fascinated Palaeozoic specialists since the end of the XIX Century. The magnificent and continuous exposures, the fine preservation and relative abundance of the fossil material, and the precise and integrated biostratigraphical constraints of the units have favoured a long tradition of stratigraphical and palaeontological study in the area. Our knowledge of this geographical sector has now placed the Carnic Alps as a fundamental key-area, at least, for the Silurian and the Devonian. However, what is even more striking is that the Carnic Alps appear to have unique features in the lower Palaeozoic peri-Gondwana sector if compared with nearby areas. Among the many peculiarities, a special attention had been reserved to the exclusive colour of the rocks in the Silurian (Ferretti et al., 2012; Histon, 2012). Ferretti (2005), Ferretti et al. (2012) and Corriga et al. (2021) reported the presence of laminated structures in the form of ferruginous-coatings around skeletal fragments with a distinct stromatolitic pattern within pink to red limestones and ironstones of Silurian age. These laminations were associated with carbonaceous matter and fossilized microbial structures, suggesting therefore a microbial role in the colouring of the Silurian (Ferretti et al., 2012). Histon (2012) analysed Silurian nautiloid-bearing strata from the Cellon section and compared the peculiar colour of their enclosing sediment with coeval occurrences along northern Gondwana in order to identify related, time-specific facies (*sensu* Brett et al., 2012) such as apparent mass mortality events and cephalopod limestone biofacies.

The Ordovician represents a remarkable interval of the Phanerozoic. The Period started with a major pulse of biodiversification (known as the Great Ordovician Biodiversification Event, or GOBE; Servais and Harper, 2018) and closed with a massive extinction, triggered by extensive glacial activity (Delabroye and Vecoli, 2010). The Late Ordovician preserved at high latitudes along the peri-Gondwana margin commonly offers only a fragmentary view of the closing part of the period due to discontinuities, associated to the onset of the Hirnantian glaciation and resulting eustatic shifts. The Upper Ordovician facies layout in the Carnic Alps was strongly influenced by basin bathymetry, especially at the Ordovician/Silurian boundary. Erosional gaps of different amplitude resulted in sporadic documentation of the Hirnantian only in the deeper parts of the basin and in a diachronous record of post-

☆ Corresponding editor: Thomas Servais.

* Corresponding authors.
E-mail addresses: ferretti@unimore.it (A. Ferretti), barbara.cavalazzi@unibo.it (B. Cavalazzi).

https://doi.org/10.1016/j.geobios.2023.01.007
0016-6995/

glacial anoxic/dysoxic Silurian shales. However, the steep slope east of Cellon mountain and south of Cellon Alm has documented, at an altitude of ca. 1500 m, an almost continuous record of the Upper Ordovician, including evidence of the glacial event supported by biostratigraphical (graptolites, chitinozoans and conodonts) and chemostratigraphical ($\delta^{13}C$ HICE Excursion) data (Ferretti et al., 2023).

A major focus of this paper is to report and describe biolaminated ferruginous structures in the Upper Ordovician Uqua Fm. of the Cellon section, and clarify the connection of this occurrence with penecontemporaneous beds inside and outside the Carnic Alps.

2. Geological setting

The Carnic Alps are a mountain chain exposed along the border between southern Austria and northern Italy in a west-east direction. Here, one of the most complete Palaeozoic successions, ranging in age from the? Cambrian/Early Ordovician to the Late Permian, is exposed over a length of ca. 110 km and a width of ca. 15 km (Ferretti et al., 2023; Fig. 1(A)). Rocks up to the Lower Pennsylvanian constitute the so-called Pre-Variscan sequence, whose lithostratigraphy has been recently revised with the formal introduction of 36 formations (Corradini and Suttner Eds., 2015). For a more detailed description of the geological framework of the Carnic Alps and of the Cellon section in particular, we refer to Corradini et al. (2015, 2016), Schönlaub et al. (2017), Corriga et al. (2016, 2021) and Corradini and Pondrelli (2021).

The ?Cambrian-Lower Ordovician of the Carnic Alps is mostly represented by clastic/volcanic units, passing to siltstones and fossiliferous limestones in the final part of the period. Regarding the Upper Ordovician, the 10 to 17 m thick massive limestone of the Wolayer Fm., represented by a shallow water cystoid-bryozoan packstone and grainstone (Schönlaub and Ferretti, 2015a), was deposited in the shallower parts of the Carnic basin (the area of Lake Wolayer: base of Mt. Seekopf, Valentintörl, Rauchkofel Boden sections; Schönlaub and Ferretti, 2015a; Corriga et al., 2021). Echinoderm debris, bryozoans, sparse corals, algae, conodonts and rare ostracodes and trilobites constitute the main components of the faunal association recovered from the unit. Dullo (1992) regarded this limestone as formed by the accumulation of parautochthonous bioclasts displaced from bryozoan-cystoid mounds, although the latter structures have never been found (Schönlaub and Ferretti, 2015a). The upper boundary of the Wolayer Fm. is marked by an impressive discontinuity surface, often associated to an ironstone horizon, indicating the Ordovician/Silurian boundary.

Laterally to the Wolayer Fm., the Uqua Fm. was deposited in deeper settings (Schönlaub and Ferretti, 2015b) in the form of 1.5 to 9 m thick nodular limestones documenting a bioclastic association of acritarchs, brachiopods, conodonts, cephalopods, chitinozoans, foraminiferans, gastropods, ostracods, sponge spiculae and trilobites (Schönlaub and Ferretti, 2015b). The stratotype of the Uqua Fm. is exposed in the Cellon section (Fig. 1(B)) at an avalanche gorge (Fig. 1(C, D)), where the unit reaches a thickness of ca. 7.3 m (beds 1–4 in Walliser, 1964; Fig. 1(E)) with interbeds of greenish siltstones in the upper part (member 2 in Schönlaub et al., 2011; Fig. 1(E)). The Uqua Fm. conformably passes to the grayish to blackish limestones and calcareous sandstones of the Plöcken Fm., a 1.5 to 9 m thick unit attesting a further shallowing of the basin associated with the onset of the Hirnantian glaciation (Schönlaub and Ferretti, 2015c). The unit has a thickness of 6.17 m at the Cellon stratotype (beds 5–8 in Walliser, 1964; Fig. 1(E)), where brachiopods of the *Hirnantia* Fauna have been documented at levels 5 (associated with *Metabolograptus persculptus*; Štorch and Schönlaub, 2012) and 6 (Jaeger et al., 1975). Other fossil occurrences are represented by acritarchs, bivalves, cephalopods, chitinozoans, conodonts, echinoderms, foraminifers, gastropods, ostracodes, sponge spiculae and trilobites (Ferretti et al., 2023). A distinctive carbonate $\delta^{13}C$ excursion at the contact between the Uqua and Plöcken formations has been correlated with the HICE carbonate $\delta^{13}C$ peak (Bergström et al., 2009), confirming the Hirnantian age of the Plöcken Fm. (Schönlaub et al., 2011). K-bentonites levels (asterisks in the Cellon log; Fig. 1(E)) were described and discussed by Histon et al. (2007) and represent a further tool for global correlation outside the Carnic basin. Glacial evidences are represented by diamictites, channeling, erosion and local non-deposition (Schönlaub, 2000; Schönlaub et al., 2011; Hammarlund et al., 2012).

Corriga et al. (2021) recently revised the Ordovician/Silurian boundary in the Carnic Alps with new conodont biostratigraphical data. The boundary unconformably truncates the Wolayer or Plöcken formations with a hiatus, embracing the latest Ordovician and the earliest Silurian, that becomes significantly larger when passing from the deeper (Bischofalm facies; *sensu* Schönlaub, 1971) to the shallower part of the Carnic basin (Wolayer facies; *sensu* Schönlaub, 1971). The Silurian onlap appears to be directed in the central sector of the Carnic Alps from south-east to north-west in a general ramp-type setting (Corriga et al., 2021).

3. Material and methods

3.1. Material

This study is based upon a large set of samples collected in a series of fieldwork excursions over the last 15 years, associated with a detailed taphonomic study run directly in the field with the intention to decipher stratigraphy and tectonic overprints. Bed-by-bed description and sampling was run of the Wolayer, Uqua and Plöcken formations in their main exposures (Rauchkofel Boden, base of Mt. Seekopf, Seewarte, Valentintörl, Cellon, Rifugio Nordio and Valbertad sections). Conodont contents were carefully checked in order to have a precise biostratigraphical setting of each horizon. Material described in the present study derives from the Cellon section. Sample preparation was undertaken in the laboratories of the Department of Chemical and Geological Sciences of the University of Modena and Reggio Emilia, Italy, resulting in 40 uncovered polished 45 mm × 60 mm thin-sections from the Uqua (levels Cellon 1, 2, above 2, 3, 4 and 4A) and Plöcken (levels Cellon 5, 6, 7, 8 base and 8 top) formations (Fig. 1(E)).

Lithological samples and thin sections are housed in the "Inventario Paleontologia Università di Modena e Reggio Emilia (IPUM)" at the Department of Chemical and Geological Sciences, University of Modena and Reggio Emilia, Italy.

3.2. Age control of the material

The Upper Ordovician calcareous units of the Carnic Alps have been used for detailed conodont studies at least in southern Europe and have allowed precise biostratigraphical framing of the succession, integrated by graptolite (Jaeger, 1975; Jaeger et al., 1975) and chitinozoan (Priewalder, 1987, 1997) data. Walliser (1964), in his fundamental paper for Silurian conodont biostratigraphy from the Cellon section, reserved a brief description to the Ordovician "Bereich I". The pioneer papers of Enrico Serpagli (Serpagli and Greco, 1965a, b; Serpagli, 1967), funded on the Italian exposures of the Uqua Fm., provided a comprehensive and detailed view of the Late Ordovician conodont fauna, however still applying the morphospecies concept. Additional data were supplemented by Manara and Vai (1970), Schönlaub (1971), Vai and Spalletta (1980), Bagnoli et al. (1998, 2017), Schönlaub et al. (2017).

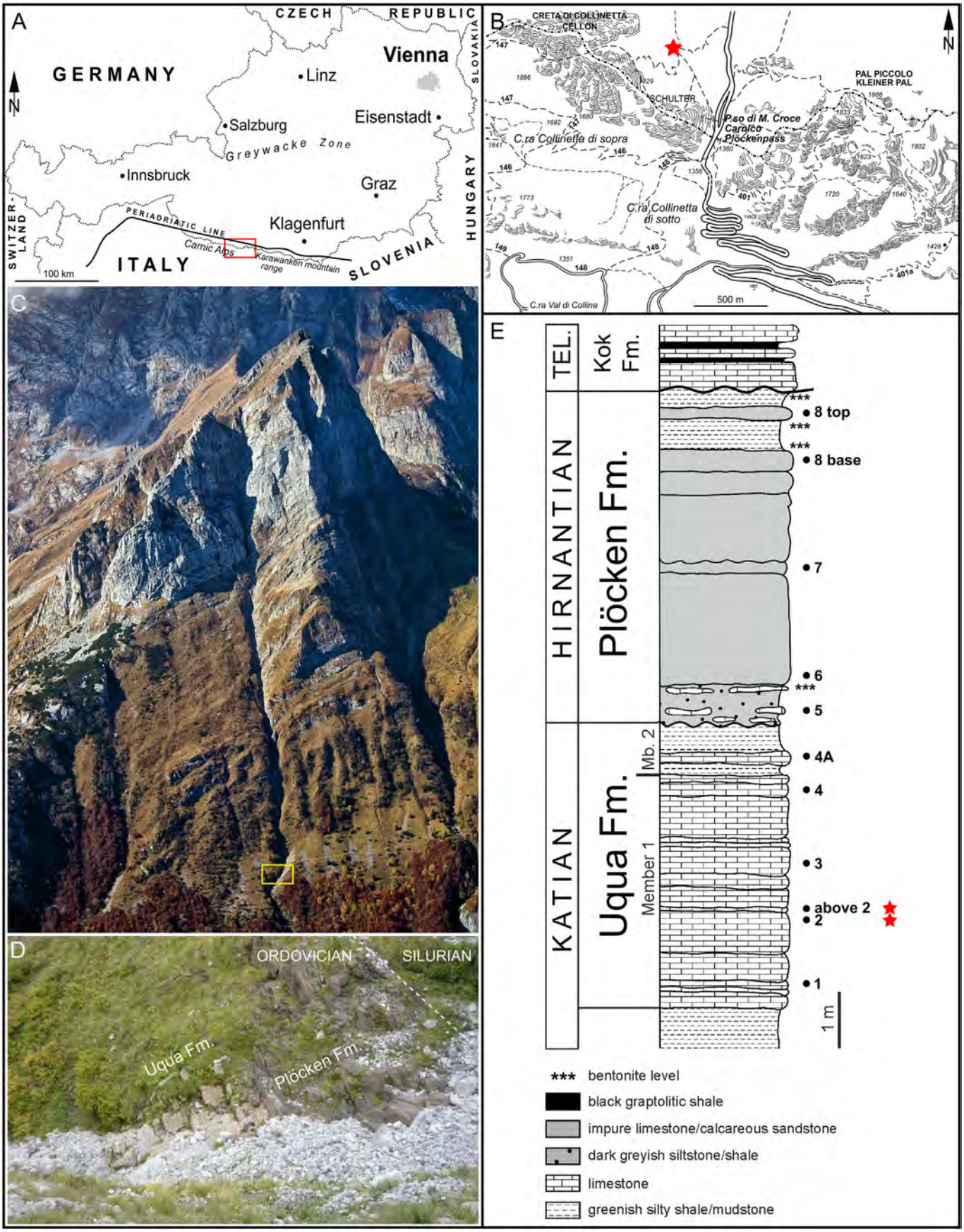

Fig. 1. A, B. Location map of the area investigated in this study. The inset in A is detailed in B. Red star in B marks the position of the Cellon section. **C, D.** General view of the Cellon section in aerial panoramic view (C: credit R. Hombacher Arosa) and detail of the Ordovician outcrop showing the Uqua and Plöcken formations and the Ordovician/Silurian boundary in D (inset in C). **E.** Stratigraphic log of the Ordovician part of the Cellon section (modified after Schönlaub et al., 2011). Red stars indicate horizons that have documented the biolaminated structures detailed in this study.

Ferretti and Schönlaub (2001), after detailed sampling of the key-areas, described the conodont association from the Wolayer Fm. in several sections around the Wolayer lake and from the Uqua and Plöcken formations in the Cellon section. All units were demonstrated to contain the *Amorphognathus ordovicicus* Biozone, thus confirming a Late Ordovician age (Ferretti and Bergström, 2017). Ferretti et al. (2014) and Bergström and Ferretti (2015) recently revised historical Ordovician localities in the United Kingdom, and finally assigned to *Amorphognathus duftonus* Rhodes, 1955 the holodontiform elements of the genus with the typical barb-like denticle, defining in this way the full architecture of the apparatus. According to those studies, the holodontiform elements described from the Carnic Alps by Serpagli (1967) belong to *Amorphognathus duftonus*, reported from the Wolayer, Uqua and Plöcken formations.

Even more importantly, the Plöcken Fm. provided a moderately-rich Hirnantian conodont fauna, the first ever recovered in Europe, documenting for the first time also the response of conodonts to the initial phase of the Late Ordovician extinction event (Ferretti and Schönlaub, 2001; Ferretti et al., 2023).

3.3. Analytical methods

Thin sections were described using optical and scanning electron microscopy (SEM), as well as environmental scanning electron microscopy coupled with microanalyses (SEM/ESEM-EDX), and a confocal laser Raman microscope.

Thin sections were initially investigated by using a transmitted and reflected optical light microscope, a Jenapol microscope equipped with a Canon EOS 350D (at the UNIMORE, Italy).

Subsequently, Au-coated and uncoated thin sections, mounted on aluminium stubs previously covered with carbon-conductive adhesive tape, were analysed (at the UNIMORE, Italy) with an Environmental Scanning Electron Microscope FEI ESEM-Quanta 200, equipped with an Oxford EDX INCA 300 X-ray energy dispersive spectrometer system, and a Scanning Electron Microscope Nova Nano SEM FEI 450, equipped with a X-EDS Bruker QUANTAX-200 detector. ESEM observations were conducted in High and Low Vacuum (LV: 1 and 0.5 Torr). Scanning electron microscope observations were performed under High Vacuum with an accelerating voltage from 15 to 25 keV both for imaging and elemental analyses.

Raman spectroscopy was performed (at the CBM-CNRS, France) using a WITec Alpha500 RA spectrometer with a frequency doubled Nd:YAG green laser (wavelength 532 nm). The system is equipped with a motorized displacement stage permitting to scan the sample and to obtain hyperspectral dataset. Data processing then enables to create concentration and composition maps, or to extract the average spectrum of a specific phase (Foucher et al., 2017). For this study, hyperspectral data were acquired using a Nikon E Plan 20 × objective (NA = 0.40) and a laser power of 13 mW at surface. This relatively high laser power was required to obtain a sufficient signal to noise ratio; nevertheless, such a power is known to transform goethite into hematite (Foucher, 2021). Average spectrum of each phase was obtained from the maps using different masks, cosmic rays removal, background subtraction and deconvolution. Additional Raman spectra were acquired by spot analyses using a laser power of 4.5 mW on specific phases.

4. Results

4.1. Microfacies description

Six levels were sampled from the Uqua Fm. (Cellon 1, 2, above 2, 3, 4 and 4A; Fig. 1(E)), covering the full exposure of the unit in the Cellon section. Only the lower part of the formation (levels Cellon 2 and Cellon above 2) revealed the presence of reddish to greenish laminated structures that coat the bioclasts. These ferruginous constructions were not detected elsewhere in the coeval levels of the Wolayer Fm. or in the overlying Hirnantian Plöcken Fm. at Cellon.

Level Cellon 2 was sampled at the top of the massive calcareous bed 2 in Walliser (1964); level Cellon above 2 is a 10 cm horizon exposed immediately above (Figs. 1(E), 2(A, B)). In thin section, level Cellon 2 is represented either by light-gray nodular deposits of equidimensional biodebris scattered within a darker matrix (Fig. 2(E, F)) or by monotonous micritic deposition with sparse trilobites and echinoderms (Fig. 4(E)). Nodules are dominated by wackestone-packstones of articulated and disarticulated bivalves and ostracodes, gastropods, echinoderm ossicles, rare trilobites and cephalopods. Micritization (mostly of echinoderms) and umbrella effects are common (Fig. 2(E, F)). Trilobite-echinoderm wackestone has been as well documented from the same level, with trilobite and echinoderm skeletal elements dispersed in the matrix without any preferred orientation. Level Cellon above 2 is represented by a brachiopod-trilobite wackestone (Fig. 2(C, D)). The brachiopods are commonly articulated and have medium dimensions. Skeletal debris, represented by cephalopod shells, echinoderms, ostracodes, gastropods, bryozoans, and possible stromatoporoids, is associated and lacks any preferred orientation (Fig. 3(D)). Shell dissolution and dolomitization is common.

4.2. Ferruginous laminated structures

The ferruginous laminated structures described in this study were recorded in the more micritic levels of the wackestone, and appear to be lacking in the nodular bioclastic horizons. Coated material represents a minor part of the fauna documented in thin section (Figs. 3(D), 4(E)). Trilobites seem to be the most common skeletal elements to be coated, with a few subordinate cephalopod shells. Laminated coatings may be incomplete, consisting of multiple layers growing on parts of the shell, or they may envelope the entire organism. These structures mostly grow starting from prominent parts of the shell or from the shell extremity (Fig. 3(C)). Coatings consist of a series of small domes developed only on the external part of the shell and exhibiting a fabric of alternating lamination of white laminae, with individual sparry laminae up to 30 μm thick, and dark yellow to green to red laminae. Laminae are more or less continuous. Reddish laminae are more difficult to discriminate especially at larger magnification where they often reveal a spotty fabric (Fig. 4(B)). Analogous alternating patterns occur in adjacent domes, as evidenced by white laminae that occupy the same position and with a comparable thickness in close bulges (Fig. 4(C)). This suggests a simultaneous evolution of the coating in the diverse domes. The outer shell margin of coated trilobites (Fig. 3(C)) and cephalopods (Fig. 5(A)) often reveals external dissolution and/or bioerosion, as well as traces of microborings.

SEM/ESEM-EDX analyses of the reddish laminae revealed the association of Fe and O, suggesting the presence of goethite. Greenish laminae within micro-domes (Fig. 5(A)) are characterised by the concurrent increase of Fe, Si, Al and Mg, indicating the probable occurrence of chamosite, a phyllosilicate that has already been reported in the Silurian counterpart. At the same time, white laminae alternating with the iron-phases documented the increase of Ca and C (Fig. 5(E)).

The Raman map of the Cellon 2 reddish laminae (Fig. 4(B)) displayed in Fig. 6(B) shows the presence of ubiquitous calcite with quartz and albite grains in the mineral matrix as well as the recovery of significant small particles of carbonaceous matter. The Raman spectra of these laminae also display an additional band around 400 cm^{-1} (Fig. 6(C)) attributed using spot analysis to

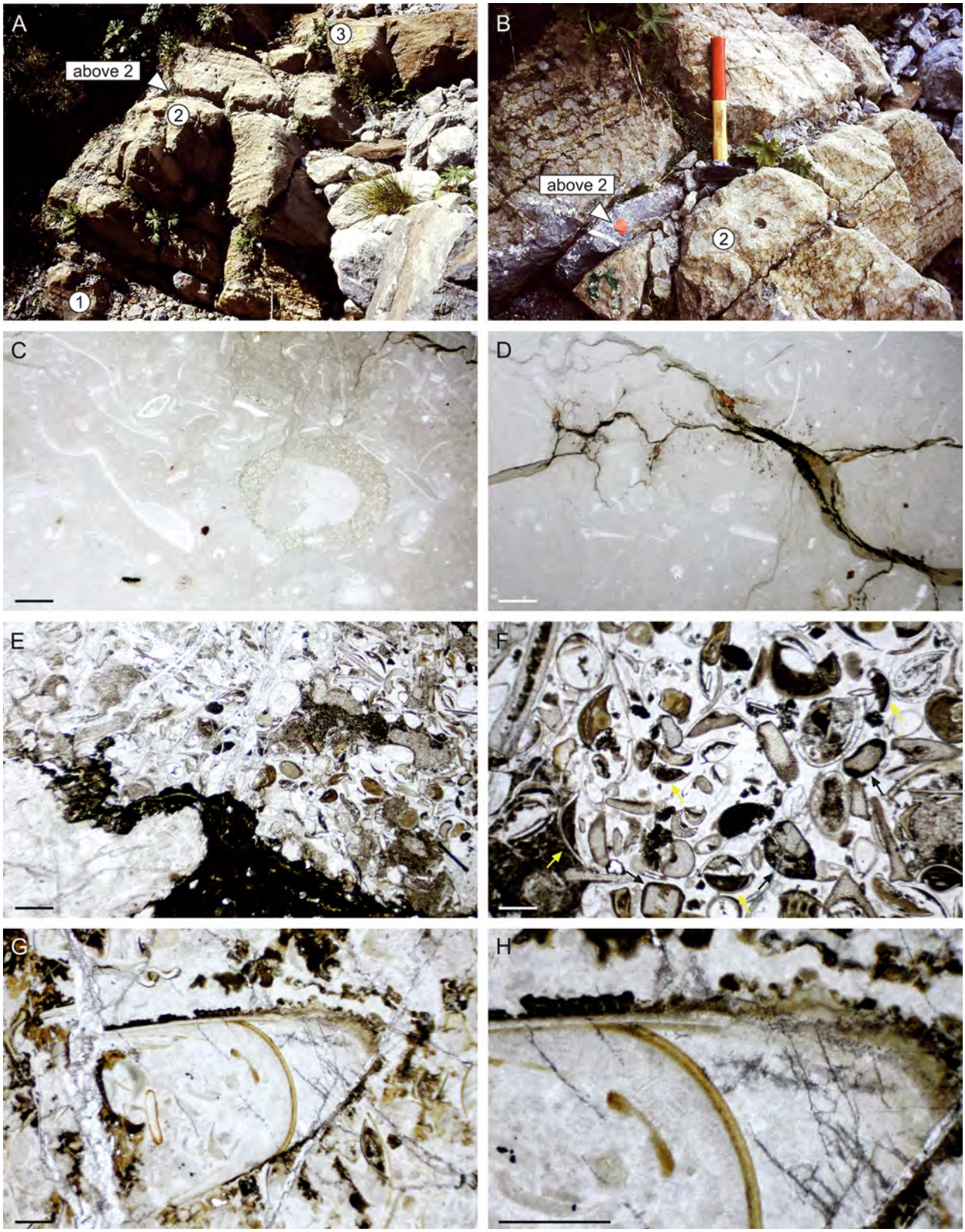

Fig. 2. A, B. Close views of the lower part of the Cellon section exposing the Uqua Formation with indication of the sampled horizons. **C–H.** Transmitted-light micrographs of petrographic thin sections illustrating main microfacies of the Uqua Formation from the Cellon section. C, D: Level Cellon above 2. Rare trilobites and echinoderm debris are sparse in a nodular fossiliferous mudstone; E, F: Level Cellon 2. Bioclastic wackestone with accumulation of equidimensional echinoderm ossicles, disarticulated bivalve shells, ostracodes, gastropods and rare trilobites. Note micritized echinoderm remains (black arrows) and umbrella effects (yellow arrows); G, H: Level Cellon 2. Incipient ferruginous coating developed around a nautiloid skeletal fragment (detailed in H). Note the laminated and multi-columnar fabric of the structure. Scale bars: 1 mm (C–E), 500 μm (F–H).

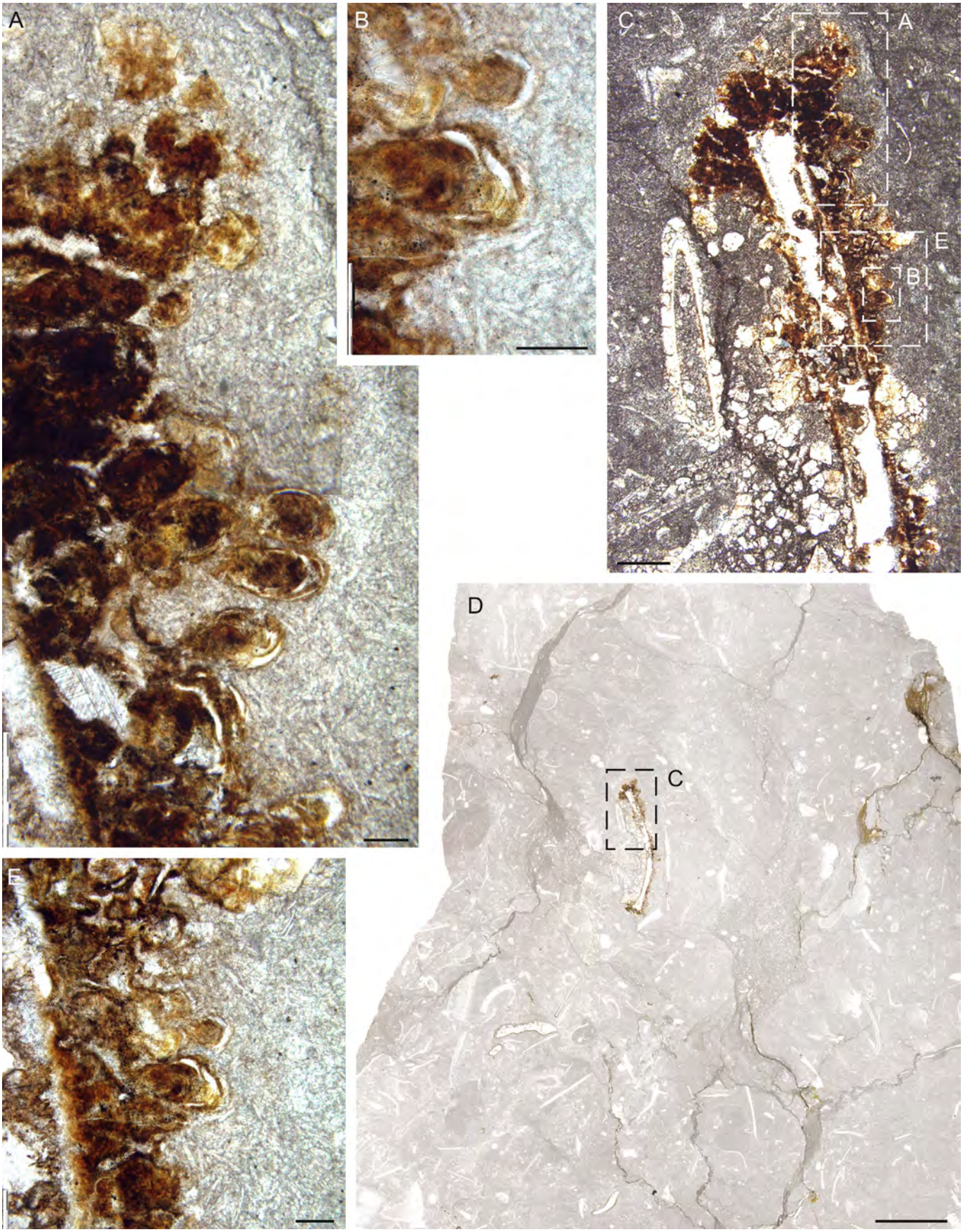

Fig. 3. A–E. Level Cellon above 2. Laminated bio-ironstones in the form of ferruginous microstromatolites growing around a trilobite skeletal fragment. Insets A, B and E detail the columnar fabric of the ferruginous coating and the alternation of calcite and Fe oxyhydr-/oxides producing the peculiar rusty colour. Note how structures are more developed at the trilobite margin (C). Scale bars: 100 μm (A, B, E), 500 μm (C), 5 mm (D).

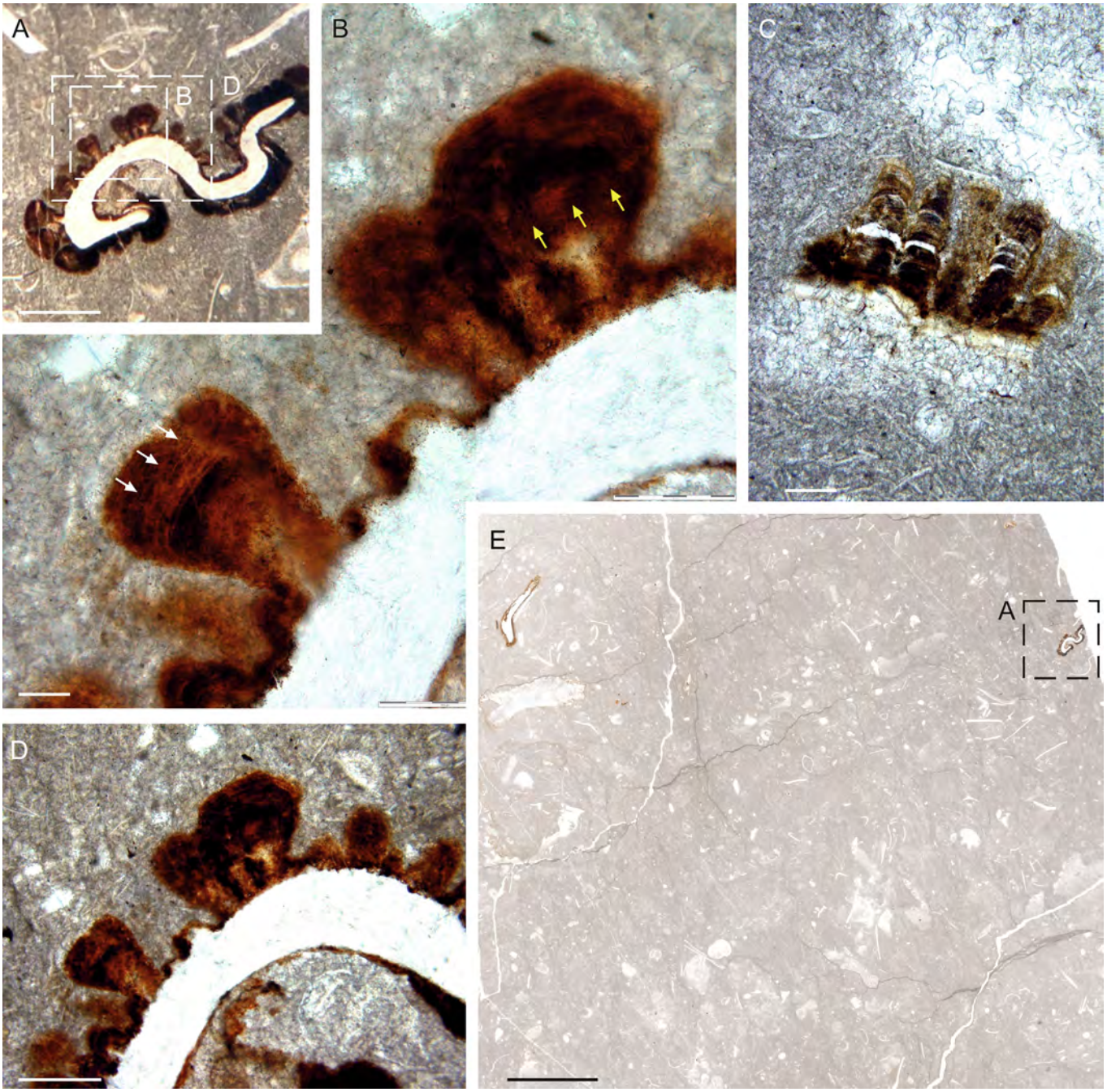

Fig. 4. Level Cellon 2. **A, B, D, E.** Trilobite skeletal elements in a fossiliferous wackestone and details of the laminated and columnar fabric of the ferruginous coating. Note how the laminated fabric is visible only in some domes (white arrows) while others are apparently indistinct (yellow arrows). **C.** Reworked and abraded microstromatolite around an undetermined skeletal fragment documenting a similar growing pattern in the diverse columnar structures developed around the outer margin. Scale bars: 500 μm (A), 200 μm (B–D), 5 mm (E).

goethite, but now in the form of hematite due to the high laser power required to collect the signal (Foucher, 2021). The Raman map of the Cellon 2 cephalopod illustrated in Fig. 5 is displayed in Fig. 6(E). It is characterised by a higher background level (lower signal to noise ratio). Nevertheless, it is possible to detect hematite (previously goethite), calcite and carbonaceous matter.

5. Discussion

Kreutzer (1990, 1992) provided a first study of the Ordovician to Devonian microfacies exposed in the Central Carnic Alps, reporting the presence of a peculiar laminated fabric around cephalopod shells, interpreted as of algal origin, in the Silurian part of the Cellon section. Later, Ferretti et al. (2012) focused on ferruginous structures documented in diverse Silurian sections of the Carnic Alps and discriminated three distinct types of bio-mediated iron-rich structures: (*i*) ferruginous "stromatolite-like" laminar structures mostly developed in correspondence to significant stratigraphic gaps, (*ii*) localized iron ooids, and (*iii*) ferruginous coatings around skeletal fragments (mostly trilobites, cephalopods and echinoderms). As regards the latter, the entire faunal association of one location (Valentintörl Section 1) was totally constituted by coated benthic organisms (dominant trilo-

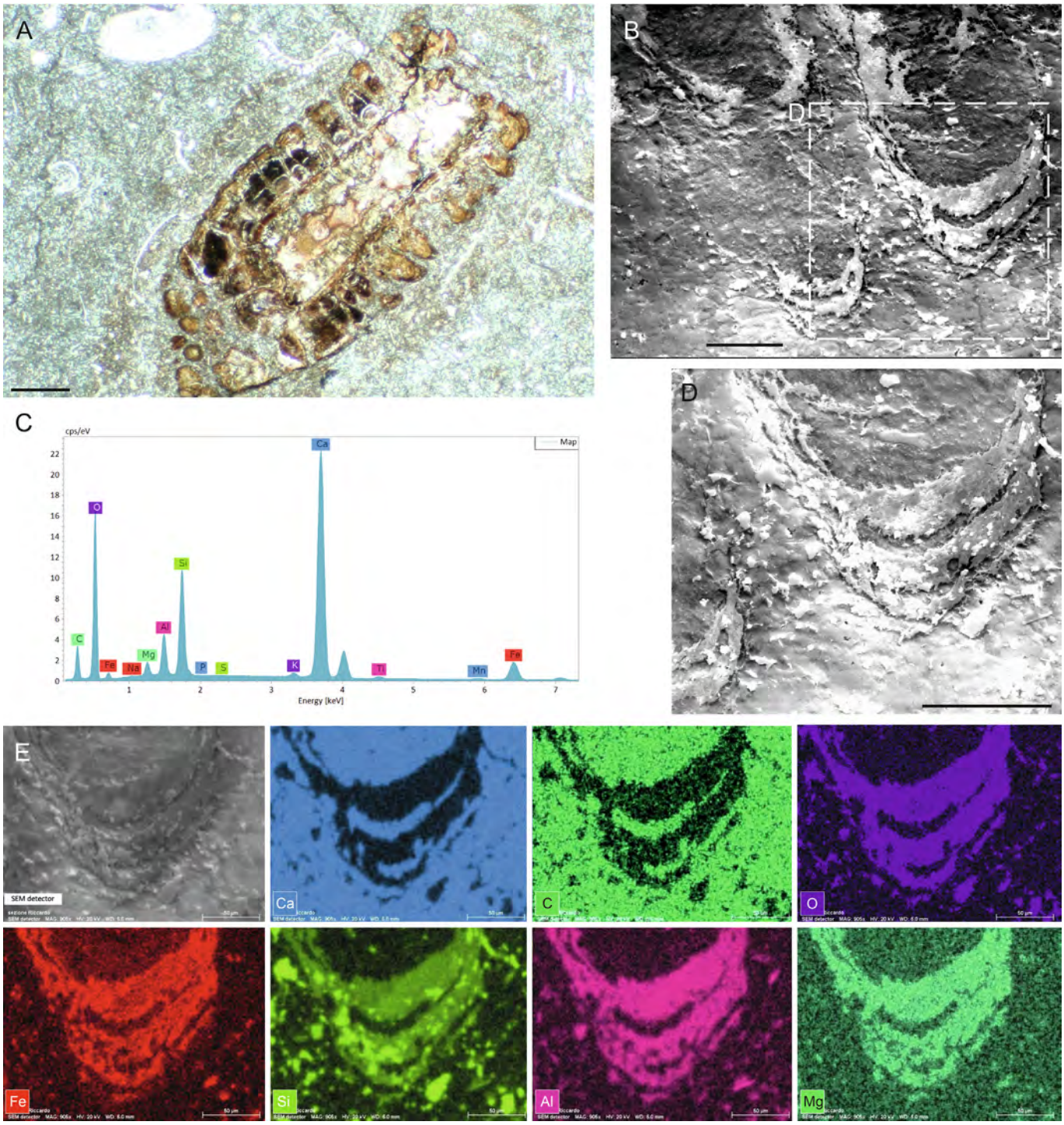

Fig. 5. Level Cellon 2. **A.** Cephalopod exposing a complete ferruginous multi-columnar coating around the shell. **B–D.** Scanning electron micrographs (B, D) and spectrum (C) of the laminated coating. **E.** SEM–EDS elemental maps (Ca, C, O, Fe, Si, Al and Mg) of the columnar structure framed in D. Note the joined increase of Fe, Si, Al and Mg and the concurring decrease of Ca and C. Scale bars: 500 μm (A), 50 μm (B, D).

bites and subordinate bryozoans) and possibly represented the source area where coating occurred. From there, coated bioclasts were redeposited at deeper settings in near-by locations, where intermixed coated and uncoated skeletal grains were documented. Goethite, magnetite, hematite, chamosite, calcite and subordinate apatite created spectacular dark red, green, white and brownish ferruginous laminae. Such iron-enrichments characterized three specific time frames of the Silurian, documenting episodes of microbial activity able to metabolize the iron present in the environment in form of "bio-ironstones" (ferruginous microstromatolites and Fe-multilayered mineralized structures). These time-specific facies can be followed around different basins (Brett et al., 2012; McLaughlin et al., 2012) and reflect episodes of global extension. Brett et al. (2012) discussed these iron-enrichments as chemical events and condensation-related time-specific facies.

The Late Ordovician of the Carnic Alps documents a change from a siliciclastic to a carbonate-dominated sedimentation (Uqua

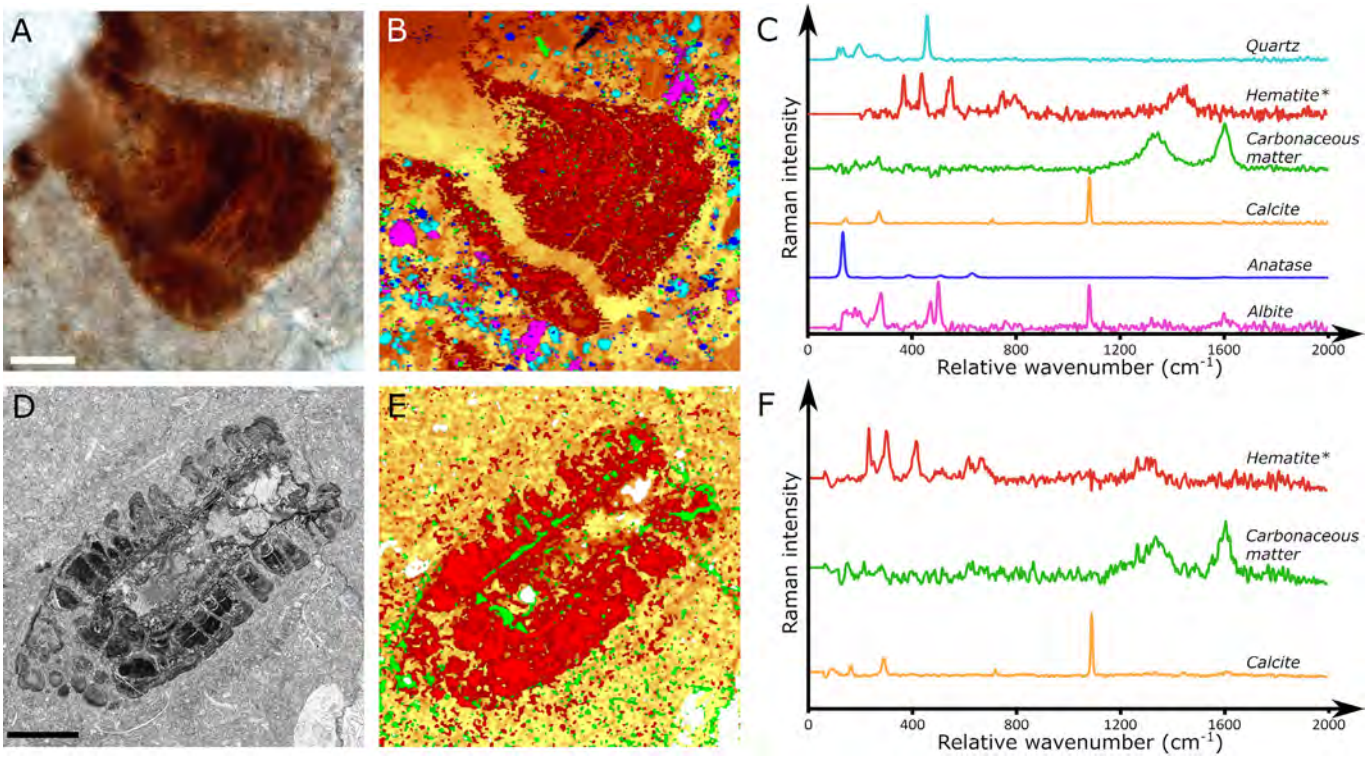

Fig. 6. Level Cellon 2. **A–C.** Optical image in transmitted light (A) and associated compositional Raman map (B) with calcite in orange/yellow, carbonaceous matter in green, anatase in dark blue, quartz in light blue, albite in fuchsia and hematite (initially goethite) in red of the laminated structure displayed in Fig. 4(B). Associated Raman spectra (C) obtained from the map, except Raman spectrum of hematite obtained from single spot analyses. **D–F.** Optical image in transmitted light (D) and associated compositional Raman map (E) with calcite in orange/yellow, carbonaceous matter in green, and hematite (initially goethite) in red of the cephalopod structure displayed in Fig. 5(A). Associated Raman spectra (F) obtained from single spot analyses. Scale bars: 40 μm (A, B), 400 μm (D, E).

and Wolayer formations), a shift already reported in the high-latitude peri-Gondwana region as a consequence of the late Katian Boda global warming event (Ferretti et al., 2023). Our study details the occurrence of the oldest biolaminated structures ever reported in the Carnic Alps and in the entire peri-Gondwana region, specifically in the Upper Ordovician of the Uqua Fm. There, only the third type of iron-rich structure reported by Ferretti et al. (2012), that is ferruginous coatings around skeletal fragments, has been so far reported. However, ferruginous coated material represents just a subordinate fraction of the entire fauna documented in the unit. The depositional environment of the Uqua Fm., as a whole, suggests conditions of relatively calm, normal-saline marine waters in which large trilobites and brachiopods lived and where a muddy mudstone fading to wackestone was sedimenting, still in conditions of relative oxygenation as also suggested by frequent bioturbation signals. Within this environment, periodic redeposition of bioclastic material from shallower areas occurred, as evidenced by nodular bioclastic packstone of shallow-water associations and thin horizons of bryozoan wackestone to packstone, possibly derived from the bryozoan-cystoid mounds thriving in the more emerged areas around the Lake Wolayer. Transport was limited, as suggested by the still articulated shells and the lack of intense fragmentation of the skeletal material. In addition, the sparse occurrence of ferruginous laminated structures in the micritic wackestone from levels Cellon 2 and Cellon above 2 intermixed with dominant uncoated material indicate a double input of skeletal elements and the existence of a further nearby area where coating occurred (“iron factory”), diverse from the location where shallow material of the packstone was produced. In the former site grains were coated, possibly through the help of microbial activity able of detracting iron from the water, and later transported to the Cellon settings. Indications of a possible microbial mediation in the formation of the mini, columnar-like structures come from their typical, laminated columnar structure with a bulbous head. The laminae are thicker at the tops of the columns and taper down their sides. They also form in a radiating fashion around the coated bioclasts. Although carbonaceous matter is associated with these structures, it seems to be located more in the calcitic matrix. Where associated with the ferruginous coatings, e.g., Fig. 6(E), it forms a layer parallel to the outline of the bioclast (evidently part of the growth process), as well as occurring in a radiating fashion within the columns.

Conditions of normal light and sufficient but possible intermittent oxygenation in the Cellon section are suggested by the well represented benthic fauna, frequent micritization of bioclasts and common bioturbation signals. However, similar structures have been reported as well from low-light and deep settings in other time frames (Reitner, 1993; Kershaw, 2000; Kershaw et al., 2005).

Vodrážkova et al. (2022) reported ferruginous coated grains of microbial origin from the Lower Devonian of the Prague Basin (Czech Republic) and stressed, once more, how different models may concur in the genesis of ironstones during the Phanerozoic. Iron may derive from continental chemical weathering, volcanic activity or be related to black shales in anoxic waters (Vodrážkova et al. 2022). This latter suggestion is particularly appealing as organic carbon-rich layers associated with anoxic waters accumulated in intervals that overlap main periods of ironstone deposition (Negri et al., 2009a, b). The recent modelling of ironstone formation in hydrothermal settings (Todd et al., 2019; Pufahl et al., 2020; Dunn et al., 2021; Matheson and Pufahl, 2021; Papazzoni et al., 2022; Vodrážkova et al., 2022) and the report of modern iron ooids at the hydrothermal scenario of Panarea (Di Bella et al., 2019, 2021; Ferretti et al., 2019) add a further possible explanation on the genesis of these ferruginous

constructions, suggesting a further perspective on the study of Phanerozoic ironstones.

Ferruginous deposits represent a time-specific facies that documents episodes of global iron-enrichments occurring in the seas. It is therefore crucial, if we want to get to a full explanation on the genesis of these iron-rich biosignatures, to expand our search inside and outside the Carnic Alps, starting from other peri-Gondwana areas (e.g., the United Arabian Emirates, unpublished material), in order to decipher what was happening in the Late Ordovician a few instants before the great glaciation developed and the mass extinction of the final period occurred.

6. Conclusions

The Uqua Fm. from the Cellon section documents the first occurrence in the Carnic Alps of Late Ordovician ferruginous structures having a distinct laminated arrangement around selected skeletal grains of Fe oxyhydr-/oxides and/or Fe-aluminosilicates alternating with calcite laminae. They represent the oldest evidence so far reported of a likely bio-mediated Fe-mineralization in the entire peri-Gondwana sector. Chamosite and goethite constitute the main iron-phases detected. The few coated materials are intermixed with dominant uncoated fossil material, suggesting a transport and redeposition from a nearby location into the depositional setting of the Cellon area. This documentation, even if represented by such a sparse report, strongly indicates the need of shifting to older times our search for the genetic conditions that enabled the construction of these biomediated ferruginous structures, that appear to get more dominant (or possibly only more easily preserved) in the Silurian and the Devonian.

Data availability

Data will be made available on request.

Declaration of Competing Interest

The authors declare that they have no known competing financial interests or personal relationships that could have appeared to influence the work reported in this paper.

Acknowledgements

Most of the material was sampled by AF together with Kathleen Histon and Hans Peter Schönlaub, which are acknowledged for their long discussions in the field, assistance and support. Reviewers Stephen Kershaw and Carlo Corradini provided insightful comments and constructive criticism that helped clarify many of our arguments. We greatly acknowledge useful observations on the manuscript by Editor-in-Chief Gilles Escarguel and Invited-Editor Thomas Servais. We express as well our deep thanks to Massimo Tonelli and Mauro Zapparoli (Scientific Instruments Facility, University of Modena and Reggio Emilia) for their technical support. This paper is a contribution to IGCP Project 735 "Rocks and the Rise of Ordovician Life".

References

Bagnoli, G., Ferretti, A., Serpagli, E., Vai, G.B., 1998. Late Ordovician conodonts from the Valbertad section (Carnic Alps). Giornale di Geologia 60, 138–149.

Bagnoli, G., Ferretti, A., Simonetto, L., Corradini, C., 2017. Upper Ordovician conodonts in the Valbertad section. Berichte des Institutes für Erdwissenschaften, Karl-Franzens-Universität Graz 23, 228–231.

Bergström, S.M., Chen, X., Gutiérrez-Marco, J.-C., Dronov, A., 2009. The new chronostratigraphic classification of the Ordovician System and its relations to regional series and stages and to $\delta^{13}C$ chemostratigraphy. Lethaia 42, 97–107.

Bergström, S.M., Ferretti, A., 2015. Conodonts in the Upper Ordovician Keisley Limestone of northern England: Taxonomy, biostratigraphical significance and biogeographical relationships. Papers in Palaeontology 1, 1–32.

Brett, C.E., McLaughlin, P.I., Histon, K., Schindler, E., Ferretti, A., 2012. Time specific aspects of facies: state of the art, examples, and possible causes. Palaeogeography, Palaeoclimatology, Palaeoecology 367–368, 6–18.

Corradini, C., Suttner, T.J. (Eds.), 2015. The Pre-Variscan sequence of the Carnic Alps (Austria and Italy). Abhandlungen der Geologischen Bundesanstalt 69, 158 p.

Corradini, C., Corriga, M.G., Männik, P., Schönlaub, H.P., 2015. Revised conodont biostratigraphy of the Cellon section (Silurian, Carnic Alps). Lethaia 48, 56–71.

Corradini, C., Pondrelli, M., 2021. The pre-Variscan sequence of the Carnic Alps (Italy-Austria). Geological Field Trips & Maps 13 (2.1), 1–72.

Corradini, C., Pondrelli, M., Simonetto, L., Corriga, M.G., Spalletta, C., Suttner, T., Kido, E., Mossoni, A., Serventi, P., 2016. Stratigraphy of the La Valute area (Mt. Zermula Massif, Carnic Alps, Italy). Bollettino della Società Paleontologica Italiana 55, 55–78.

Corriga, M.G., Corradini, C., Schönlaub, H.-P., Pondrelli, M., 2016. Lower Lochkovian (Lower Devonian) conodonts from Cellon section (Carnic Alps, Austria). Bulletin of Geosciences 91, 261–270.

Corriga, M.G., Corradini, C., Pondrelli, M., Schönlaub, H.-P., Nozzi, L., Todesco, R., Ferretti, A., 2021. Uppermost Ordovician to lowermost Devonian conodonts from the Valentintörl section and comments on the post Hirnantian hiatus in the Carnic Alps. Newsletters on Stratigraphy 54, 183–207.

Delabroye, A., Vecoli, M., 2010. The end-Ordovician glaciation and the Hirnantian Stage: A global review and questions about Late Ordovician event stratigraphy. Earth-Science Reviews 98, 269–282.

Di Bella, M., Sabatino, G., Quartieri, S., Ferretti, A., Cavalazzi, B., Barbieri, R., Foucher, F., Messori, F., Italiano, F., 2019. Modern Iron Ooids of Hydrothermal Origin as a Proxy for Ancient Deposits. Scientific Reports 9, 7107.

Di Bella, M., Pirajno, F., Sabatino, G., Quartieri, S., Barbieri, R., Cavalazzi, B., Ferretti, A., Danovaro, R., Romeo, T., Andaloro, F., Esposito, V., Italiano, F., 2021. Rolling ironstones from Earth and Mars: Terrestrial hydrothermal ooids as a potential analogue of Martian spherules. Minerals 11, 460.

Dullo, W.C., 1992. Mikrofazies und Diagenese der oberordovizischen Cystoideen-Kalke (Wolayerkalk) und ihrer Schuttfazies (Uggwakalk) in den Karnischen Alpen. Jahrbuch der Geologischen Bundesanstalt 135, 317–333.

Dunn, S.K., Pufahl, P.K., Murphy, J.B., Lokier, S.W., 2021. Middle Ordovician upwelling-related ironstone of North Wales: coated grains, ocean chemistry, and biological evolution. Frontiers in Earth Science 9, 669476.

Ferretti, A., 2005. Ooidal ironstones and laminated ferruginous deposits from the Silurian of the Carnic Alps, Austria. Bollettino della Società Paleontologica Italiana 44, 263–278.

Ferretti, A., Bergström, S.M., 2017. Conodonts in Ordovician biostratigraphy. Lethaia 50, 424–439.

Ferretti, A., Cavalazzi, B., Barbieri, R., Westall, F., Foucher, F., Todesco, R., 2012. From black-and-white to colour in the Silurian. Palaeogeography, Palaeoclimatology, Palaeoecology 367–368, 178–192.

Ferretti, A., Bergström, S.M., Barnes, C.R., 2014. Katian (Upper Ordovician) conodonts from Wales. Palaeontology 57, 801–831.

Ferretti, A., Messori, F., Di Bella, M., Sabatino, G., Quartieri, S., Cavalazzi, B., Italiano, F., Barbieri, R., 2019. Armoured sponge spicules from Panarea Island (Italy): Implications for their fossil preservation. Palaeogeography, Palaeoclimatology, Palaeoecology 536, 109379.

Ferretti, A., Schönlaub, H.P., 2001. New conodont faunas from the Late Ordovician of the Central Carnic Alps, Austria. Bollettino della Società Paleontologica Italiana 40, 3–15.

Ferretti, A., Schönlaub, H.P., Sachanski, V., Bagnoli, G., Serpagli, E., Vai, G.B., Yanev, S., Radonjić, M., Balica, C., Bianchini, L., Colmenar, J., Gutiérrez-Marco, J.C., 2023. In: Harper, D.A.T., Lefebvre, B., Percival, I., Servais, T. (Eds.), A Global Synthesis of the Ordovician System Part 1. Geological Society of London Special Publication 532. https://doi.org/10.1144/SP532-2022-174.

Foucher, F., Guimbretiè, A.G., Bost, N., Westall, F., 2017. Petrographical and Mineralogical Applications of Raman Mapping. In: Maaz, K. (Ed.), Raman Spectroscopy and Applications. InTtechOpen Limited, Chapter 8, pp. 163–180.

Foucher, F., 2021. Influence of laser shape on thermal increase during micro-Raman spectroscopy analyses. Journal of Raman Spectroscopy 53, 163-180.

Hammarlund, E.U., Dahl, T.W., Harper, D.A.T., Bond, D.P.G., Nielsen, A.T., Bjerrum, C. J., Schovsbo, N.H., Schönlaub, H.P., Zalasiewicz, J.A., Canfield, D.E., 2012. A sulfidic driver for the end-Ordovician mass extinction. Earth and Planetary Science Letters 331–332, 128–139.

Histon, K., 2012. The Silurian nautiloid-bearing strata of the Cellon Section (Carnic Alps, Austria): Color variation related to events. Palaeogeography, Palaeoclimatology, Palaeoecology 367–368, 231–255.

Histon, K., Klein, P., Schönlaub, H.P., Huff, W.D., 2007. Lower Paleozoic K-bentonites from the Carnic Alps, Austria. Mitteilungen der Österreichischen Geologischen Gesellschaft 100, 26–42.

Jaeger, H., 1975. Die Graptolithenführung im Silur/Devon des Cellon-Profils (Karnische Alpen). Carinthia II 165, 111–126.

Jaeger, H., Havliček, V., Schönlaub, H.P., 1975. Biostratigraphie der Ordovizium/Silur-Grenze in den Südalpen – Ein Beitrag zur Diskussion um die Hirnantia-Fauna. Verhandlungen Geologische Bundesanstalt 1975, 271–289.

Kershaw, S., 2000. Quaternary reefs of northeastern Sicily: structure and growth controls in an unstable tectonic setting. Journal of Coastal Research 16, 1037–1062.

Kershaw, S., Guo, L., Braga, J.-C., 2005. A Holocene coral-algal reef at Mavra Litharia, Gulf of Corinth, Greece: structure, history and applications in relative sea-level change. Marine Geology 215, 171–192.
Kreutzer, L.H., 1990. Mikrofazies, Stratigraphie und Paläogeographie des Zentralkarnischen Hauptkammes zwischen Seewarte und Cellon. Jahrbuch der Geologischen Bundesanstalt 133, 275–343.
Kreutzer, L.H., 1992. Photoatlas zu den variszischen Karbonat-Gesteinen der Karnischen Alpen (Österreich/Italien). Abhandlungen der Geologischen Bundesanstalt 47, 1–129.
Manara, C., Vai, G.B., 1970. La sezione e i conodonti del costone sud del M. Rauchkofel. Giornale di Geologia 36, 441–514.
Matheson, E.J., Pufahl, P.K., 2021. Clinton ironstone revisited and implications for Silurian Earth system evolution. Earth-Science Reviews 215, 103527.
McLaughlin, P.I., Emsbo, P., Brett, C.E., 2012. Beyond black shales: the sedimentary and stable isotope records of oceanic anoxic events in a dominantly oxic basin (Silurian; Appalachian Basin, USA). Palaeogeography, Palaeoclimatology, Palaeoecology 367–368, 153–1777.
Negri, A., Ferretti, A., Wagner, T., Meyers, P.A., 2009a. Organic-carbon-rich sediments through the Phanerozoic: Processes, progress, and perspectives. Palaeogeography, Palaeoclimatology, Palaeoecology 273, 213–217.
Negri, A., Ferretti, A., Wagner, T., Meyers, P.A., 2009b. Phanerozoic organic-carbon-rich marine sediments: Overview and future research challenges. Palaeogeography, Palaeoclimatology, Palaeoecology 273, 218–227.
Papazzoni, C.A., Cavalazzi, B., Brigatti, M.F., Filipescu, S., Foucher, F., Medici, L., Westall, F., Ferretti, A., 2022. The significance of iron ooids from the middle Eocene of the Transylvanian Basin, Romania. Gondwana Research 111, 64–75.
Priewalder, H., 1987. Acritarchen aus dem Silur des Cellon-Profils, Karnische Alpen, Österreich. Abhandlungen der Geologischen Bundesantalt 40, 1–121.
Priewalder, H., 1997. The distribution of the chitinozoans in the Cellon section (Hirnantian – lower Lochkovian) – A preliminary report. In: Schönlaub, H.P. (Ed.), IGCP-421 Inaugural Meeting Vienna, vol. 40. Guidebook. Berichte der Geologischen Bundesantalt, pp. 74–85.
Pufahl, P.K., Squires, A.D., Murphy, J.B., Quesada, C., Lokier, S.W., Álvaro, J.J., Hatch, J., 2020. Ordovician ironstone of the Iberian margin: coastal upwelling, ocean anoxia and Palaeozoic biodiversity. Depositional Record 6, 581–604.
Reitner, J., 1993. Modern cryptic microbialite/metazoan facies from Lizard Island (Great Barrier Reef Australia): formation and concepts. Facies 29, 3–40.
Rhodes, F.H.T., 1955. The conodont fauna of the Keisley Limestone. Quarterly Journal of the Geological Society of London 111, 117–142.
Schönlaub, H.P., 1971. Zur Problematik der Conodonten-Chronologie an der Wende Ordoviz/Silur mit besonderer Berücksichtigung der Verhältnisse im Llandovery. Geologica et Palaeontologica 5, 35–57.
Schönlaub, H.P., 2000. The Ordovician of the Southern Alps. Mitteilungen. Österreichische Geologische Gesellschaft 91 (1998), 39–51.
Schönlaub, H.P., Corradini, C., Corriga, M.G., Ferretti, A., 2017. Chrono-, litho- and conodont bio-stratigraphy of the Rauchkofel Boden Section (Upper Ordovician-Lower Devonian), Carnic Alps, Austria. Newsletters on Stratigraphy 50, 445–469.
Schönlaub, H.P., Ferretti, A., 2015a. Wolayer Formation. In: Corradini, C., Suttner, T.J. (Eds.), The Pre-Variscan sequence of the Carnic Alps (Austria and Italy), vol. 69. Abhandlungen der Geologischen Bundesanstalt, pp. 34–37.
Schönlaub, H.P., Ferretti, A., 2015b. Uqua Formation. In: Corradini, C., Suttner, T.J. (Eds.), The Pre-Variscan sequence of the Carnic Alps (Austria and Italy), vol. 69. Abhandlungen der Geologischen Bundesanstalt, pp. 38–41.
Schönlaub, H.P., Ferretti, A., 2015c. Plöcken Formation. In: Corradini, C., Suttner, T.J. (Eds.), The Pre-Variscan sequence of the Carnic Alps (Austria and Italy), vol. 69. Abhandlungen der Geologischen Bundesanstalt, pp. 42–45.
Schönlaub, H.P., Ferretti, A., Gaggero, L., Hammarlund, E., Harper, D.A.T., Histon, K., Priewalder, H., Spötl, C., Štorch, P., 2011. The Late Ordovician glacial event in the Carnic Alps (Austria). In: Gutiérrez-Marco, J.C., Rábano, I., Garcia-Bellido, D. (Eds.), Ordovician of the World. Instituto Geológico y Minero de Espana, vol. 14. Cuadernos del Museo Geominero, pp. 515–526.
Serpagli, E., 1967. I conodonti dell'Ordoviciano superiore (Ashgilliano) delle Alpi Carniche. Bollettino della Società Paleontologica Italiana 6, 30–111.
Serpagli, E., Greco, A., 1965a. Documentazione paleontologica di Ashgilliano (Ordoviciano sup.) nel versante S del M. Zérmula (Alpi Carniche italiane). Atti e Memorie della Accademia Nazionale di Scienze, Lettere e Arti di Modena VI, 1–12.
Serpagli, E., Greco, A., 1965b. Osservazioni preliminari su alcuni Conodonti ordoviciani e siluriani delle Alpi Carniche italiane. Bollettino della Società Paleontologica Italiana 3, 192–211.
Servais, T., Harper, D.A.T., 2018. The Great Ordovician Biodiversification Event (GOBE): definition, concept and duration. Lethaia 51, 151–164.
Štorch, P., Schönlaub, H.P., 2012. Ordovician-Silurian boundary graptolites of the Southern Alps, Austria. Bulletin of Geosciences 87, 755–766.
Todd, S.E., Pufahl, P.K., Murphy, J.B., Taylor, K.G., 2019. Sedimentology and Oceanography of Early Ordovician Ironstone, Bell Island, Newfoundland: Ferruginous Seawater and Upwelling in the Rheic Ocean. Sedimentary Geology 379, 1–15.
Vai, G.B., Spalletta, C., 1980. The Uggwa section. In: Schönlaub, H.P. (Ed.), Second European Conodont Symposium. Guidebook, Abstracts, vol. 35. Abhandlungen der Geologischen Bundesanstalt, pp. 48–50.
Vodrážkova, S., Kumpan, T., Vodrážka, R., Frýda, J., Čopiaková, R., Koubová, M., Munnecke, A., Kalvoda, J., Holá, M., 2022. Ferruginous coated grains of microbial origin from the Lower Devonian (Pragian) of the Prague Basin (Czech Republic) – Petrological and geochemical perspective. Sedimentary Geology 438, 106194.
Walliser, O.H., 1964. Conodonten des Silurs. Abhandlungen des Hessischen Landes-Amtes für Bodenforschung 41, 1–106.